

**Hydrogeochemical Controls on Brook Trout Spawning Habitat in a Coastal Stream**

Martin A. Briggs<sup>1\*</sup>, mbriggs@usgs.gov, (phone) +1.860.487.7402

Judson W. Harvey<sup>2</sup>

Stephen T. Hurley<sup>3</sup>

Donald O. Rosenberry<sup>4</sup>

Timothy McCobb<sup>5</sup>

Dale Werkema<sup>6</sup>

John W. Lane, Jr.<sup>1</sup>

<sup>1</sup>U.S. Geological Survey, Hydrogeophysics Branch, 11 Sherman Place, Unit 5015, Storrs, CT, 06269 USA

<sup>2</sup>U.S. Geological Survey, Water Cycle Branch, M.S. 430, Reston, VA, 20192 USA

<sup>3</sup>Massachusetts Division of Fisheries and Wildlife, 195 Bournedale Road, Buzzards Bay, MA, 02532 USA

<sup>4</sup>U.S. Geological Survey, National Research Program, M.S. 406, Bldg. 25, DFC, Lakewood, CO, 80225 USA

<sup>5</sup>U.S. Geological Survey, 10 Bearfoot Road, Northborough, MA, 01532 USA

<sup>6</sup>U.S. Environmental Protection Agency, Office of Research and Development, National Exposure Research Laboratory, Exposure Methods & Measurement Division, Environmental Chemistry Branch, Las Vegas, NV, 89119 USA

Revised manuscript prepared for submission to *Hydrology and Earth Systems Sciences*

**Abstract:**

Brook trout (*Salvelinus fontinalis*) spawn in fall, and overwintering egg development can benefit from stable, relatively warm temperatures in groundwater seepage zones. However, eggs also are sensitive to dissolved oxygen concentration, which may be reduced in discharging groundwater (i.e. seepage). We investigated a 2-km reach of the coastal Quashnet River, Cape Cod, Massachusetts, USA, to relate preferred fish spawning habitat to geology, geomorphology, and discharging groundwater geochemistry. Thermal reconnaissance methods were used to locate zones of rapid groundwater discharge, which were predominantly found along the center channel of a wider stream valley section. Pore-water chemistry and temporal vertical groundwater flux were measured at a subset of these zones during field campaigns over several seasons. Seepage zones in open valley sub-reaches generally showed suboxic conditions and higher dissolved solutes compared to the underlying glacial outwash aquifer. These discharge zones were cross-referenced with preferred brook trout redds, evaluated during 10 yr of observation, all of which were associated with discrete alcove features in steep cut banks where stream meander bends intersect the glacial valley walls. Seepage in these repeat spawning zones was generally stronger and more variable than open valley sites, with higher dissolved oxygen and reduced solute concentrations. The combined evidence indicates that regional groundwater discharge along the broader valley bottom is predominantly suboxic due to the influence of near-stream organic deposits; trout show no obvious preference for these zones when spawning. However, the meander bends that cut into sandy deposits near the valley walls generate strong, oxic seepage zones that are utilized routinely for redd construction and the overwintering of trout eggs. Stable water isotopic data support the conclusion that repeat spawning zones located directly on preferential discharges of more localized groundwater. In similar coastal systems with extensive valley peat deposits, specific use of groundwater discharge points by brook trout

59 may be limited to morphologies such as cut banks where groundwater flowpaths do not  
60 encounter substantial buried organic material and remain oxygen rich.

## Introduction

The heat tracing of waters can be used to map a distribution of spatially focused, or “preferential”, groundwater discharge zones throughout surface water systems at times of contrast between surface and groundwater temperature. The measurement of water temperature from the reach to watershed scale is now possible using thermal infrared and fiber-optic distributed temperature sensing (FO-DTS) methodology (Dugdale, 2016; Hare et al., 2015; Steel et al., 2017). Remote infrared data collection throughout the river corridor has been enabled by handheld cameras, piloted aircraft, and the rapidly evolving capabilities of Unmanned Aircraft Systems. Researchers are capitalizing on the ongoing refinement of these technologies to identify zones of focused groundwater seepage to streams to map potential discrete preferential coldwater fish habitat such as summer thermal refugia (Dugdale et al., 2015). However, surface thermal surveys alone do not indicate groundwater flowpath dynamics or the suitability of interface aquatic habitat (Briggs et al., 2018a).

For example, dissolved oxygen (DO) concentration must be sufficiently high for cold groundwater seepage to provide support for fish life-processes at the direct point of discharge to surface water (Ebersole et al., 2003), which is not apparent from thermal analysis alone. During summer warm periods in systems with suboxic groundwater, coldwater fish species such as salmonids can face a tradeoff between occupying discrete zones of preferred water temperatures with near-lethal DO levels, or stream sections that are too warm for long-term survival (Mathews and Berg, 1997). The use of groundwater upwelling zones as thermal refugia is further complicated by competition with aggressive invasive species (to the Northeastern USA) such as brown trout that compete with native trout for resources (Hitt et al., 2017). Streams at higher elevations may support reach-scale cold water habitat where point-scale thermal refugia are not

needed under current climatic conditions, serving as vital “climate refugia” against rising air temperatures (Isaak et al., 2015). In systems with reliably cold channel water in summer, which can also exist at low elevations when heavily influenced by discharging groundwater, salmonid fish may directly use groundwater seepage zones for spawning rather than thermal refuge.

Brook trout (*Salvelinus fontinalis*) are a species of char that are native to eastern North America, from Georgia to Quebec (MacCrimmon and Campbell, 1969). Populations have been stressed by warming temperatures and reduced water quality, particularly in low-elevation areas (Hudy et al., 2008). Stream network-scale tracking of fish has indicated brook trout directly utilize stream confluence mixing zones and preferential groundwater discharge to survive warm summer periods (Baird and Krueger, 2003; Petty et al., 2012; Snook et al., 2016). Additionally, brook trout spawn in the fall, and eggs deposited in redds develop over the winter before hatching in spring (Cunjak and Power, 1986). Oxygen use by the shallow buried embryos increases over the period of development (Crisp, 1981), and therefore DO concentration is a critical parameter of the pore waters in which the eggs are bathed. Several studies have demonstrated the importance of hyporheic downwelling in increasing shallow oxygen concentrations specifically at salmonid redds when streambed pore water is generally reduced in DO (e.g. Buffington and Tonina 2009; Cardenas et al. 2016). Fine sediments can reduce the efficacy of hyporheic DO exchange in spawn zones (Obruca and Hauer, 2016), and are actively cleared by trout during the spawning process ((Montgomery et al., 1996).

The importance of hyporheic exchange to salmonid spawning may be limited in the lowland streams that are expected to harbor native cold-water species in the 21<sup>st</sup> century: those with strong groundwater influence. Groundwater upwelling reduces the penetration of hyporheic flow from surface water (Cardenas and Wilson, 2006) and may shut down hyporheic flushing in

redds (Cardenas et al., 2016). Where hyporheic exchange does introduce oxygenated channel water into the shallow streambed, the downward advection of heat associated with near-freezing surface water in winter will also cool streambed sediments (Geist et al., 2002), potentially impairing egg development. Coaster brook trout, a life-history variant of native brook trout exhibiting potadromous migrations within the Great Lakes, have been shown to specifically prefer groundwater discharge zones for building redds (Grinsven et al., 2012). The development of trout in winter has been found to be positively correlated with warmer stream water temperatures as influenced by groundwater seepage (French et al., 2016), and therefore spatially discrete groundwater discharge zones with adequate DO may form preferred brook trout spawning habitat (Curry et al., 1995).

Multiscale physical and biogeochemical factors influence temperature and DO concentrations along groundwater flowpaths. In river valleys, discharge to surface water of locally recharged groundwater is expected to emanate from more shallow, lateral flowpaths controlled by local topography (Modica, 1999; Winter et al., 1998). Shallow groundwater flowpaths, particularly those within approximately 5 m of the land surface, will be more sensitive to annual air temperature patterns and longer term warming trends due to strong vertical conductive heat exchanges (Kurylyk et al., 2015b). The distance of seeps from upgradient groundwater recharge zones will also affect seepage temperature dynamics and associated aquatic ecosystems due to future changes in surface and recharge temperature (Burns et al., 2017). Therefore, working backwards from thermal anomalies into the landscape is critical to understanding the thermal stability of current and future point-scale preferential brook trout habitat (Briggs et al., 2018b). The complimentary methodology of geophysical remote sensing, geochemical sampling, and vertical bed temperature time series can indicate the physical and

chemical properties of groundwater flowpaths that source preferential discharge zones utilized routinely by fish for spawning.

Coarse-grained mineral-dominated aquifers with little fine particulate organic matter and low dissolved organic carbon supply tend to result in generally oxic groundwater conditions (Back et al., 1993). The sandy surficial aquifer of Cape Cod, where our investigation took place, is a classic example of a mineral soil-dominated flow system (Frimpter and Gay, 1979). Flow of groundwater through near-stream organic deposits, however, can result in inverted redox gradients toward the upwelling interface, such that groundwater discharged to surface water is reduced in DO (Seitzinger et al., 2006). In sandy glacial terrain with superimposed peatland deposits, the specific flow patterns of groundwater to surface water in relation to buried peat will influence groundwater discharge biogeochemistry. Krause et al. (2013) found that streambed groundwater seepage was strongly reduced in DO in zones with peat deposits, likely due to an increase in both near-stream residence time and localized source of dissolved organic carbon.

Interdisciplinary collaborations between physical and biological scientists are useful to better understand how cold-water species utilize groundwater discharge-influenced stream habitat, and the larger landscape-scale controls on discharge characteristics. While previous hydrogeological research in the coastal stream used for this study had focused on locating and quantifying discrete groundwater discharge (e.g. “cold anomalies”, Hare et al., 2015; Rosenberry et al., 2016), here we endeavor to understand the hydraulic and biogeochemical controls on seepage zone distribution utilized directly by native brook trout. In this groundwater-dominated stream (e.g. likely climate refugia), brook trout do not need to occupy discrete inflows for summer thermal refugia, but do favor certain upwelling zones for fall spawning. We compare over a decade of visual survey and electronic fish PIT-tag dropout data regarding repeat brook

153 trout spawning locations to a comprehensive physical and chemical characterization of  
154 groundwater seepage zones across 2-km of stream to:

155 1. Identify repeat brook trout spawning locations, and determine if they are directly  
156 associated with the preferential discharge of groundwater through interface sediments.

157 2. Develop a hydrogeochemical characterization of trout-preferred groundwater discharge  
158 zones that can aid in their identification in other less-studied systems and potential  
159 inclusion in stream habitat restoration efforts.

## 160 **Site Description and Previous Hydrogeologic Characterization**

161 Cape Cod is a peninsula in southeastern coastal Massachusetts, USA, composed  
162 primarily of highly permeable unconsolidated glacial moraine and outwash deposits. The largest  
163 of the Cape Cod sole-source aquifers occupies a western (landward) section of the peninsula  
164 (LeBlanc et al., 1986), and is incised by several linear valleys that drain groundwater south to the  
165 Atlantic Ocean via baseflow-dominated streams (Figure 2a). Strong groundwater discharge to  
166 one such stream, the Quashnet River, supports a relatively stable flow regime that has averaged  
167  $0.49 \pm 0.15$  (SD)  $\text{m}^3 \text{s}^{-1}$  from 1986-2015 (Rosenberry et al., 2016). The lower Quashnet River  
168 emerges from a narrow sand and gravel valley to a broader area with well-defined lateral  
169 floodplains. Historical cranberry farming practices, abandoned in the 1950s, have modified the  
170 stream corridor (Barlow and Hess, 1993). Primary modifications included straightening of the  
171 main channel (reducing natural sinuosity), installation of flood-control structures, incision of  
172 shallow groundwater drainage ditches in the lateral peatland floodplain, and widespread  
173 application of sand to the floodplain surface. The current bank-full width of the main channel  
174 averages approximately 4 m.



The Quashnet River has long been recognized as critical habitat for a naturally reproducing population of native sea-run brook trout (Mullan, 1958) with a genetically distinct population (Annett et al., 2012). Efforts to restore trout habitat by the group *Trout Unlimited* and others have been ongoing for over 40 yr (Barlow and Hess, 1993). These efforts include the removal of flood-control structures and planting of trees along the main channel, and addition of wood structures to stabilize banks and provide cover from airborne predators. Further, the Commonwealth of Massachusetts purchased 12.5 hectares in 1956 and an additional 146 hectares along the lower Quashnet River in 1987 and 1988 to protect the area from development. The Massachusetts Division of Fisheries and Wildlife has been monitoring trout populations since 1988 and movement since 2007.

Groundwater influence on stream temperature is pronounced, particularly over the 2-km reach above the USGS gage (Briggs et al., 2018a), below which stream stage is tidally affected. Ambient regional groundwater temperature is approximately 11 °C (Briggs et al., 2014), and strong conductive and advective exchange with the proximal aquifer maintains surface water temperature well below the lethal threshold for brook trout (maximum weekly average temperature >23.3 °C, Wehrly *et al.* 2007). Therefore point-scale thermal refugia are not a current concern in this system, as the stream supports system-scale cold-water habitat that is likely to persist into the future and serve as warming “climate refugia” (Briggs et al., 2018a). In winter, seepage zones can be located as relatively warm anomalies increasing and buffering surface water temperatures from ambient atmospheric influence.

Previous work has measured relatively large net gains in streamflow over the lower Quashnet River (Barlow and Hess, 1993; Rosenberry et al., 2016), attributed to groundwater discharge through direct streambed seepage and harvesting of groundwater from the floodplain platform

via relic agricultural drainage ditches. Deployments of fiber-optic temperature sensing (FO-DTS) cables along the thalweg streambed interface indicate the greatest density of focused seepage zones occurs along the broader valley area approximately 1 km upstream of the USGS gage number 011058837; this zone coincides with the largest gains in net streamflow (Hare et al., 2015). Based on the streambed interface temperature data presented by Rosenberry et al. (2016), Figure 1 shows how temperature-sensitive fiber optic cables have been used to pinpoint possible groundwater discharge zones based on anomalously cold mean temperature and/or reduced thermal variance. Focused evaluation of FO-DTS anomalies with physical seepage meters and vertical temperature profilers confirmed localized, meter-scale seepage zonation along the streambed where discrete colder zones indicated through heat tracing showed approximately 5 times the groundwater discharge rate of adjacent sandy bed locations only meters away (Rosenberry et al., 2016). Active heating of wrapped FO-DTS cables deployed vertically within an open valley streambed seepage zone indicated true vertical flow to at least 0.6 m into the bed sediments (Briggs et al., 2016), an expected characteristic of more regional groundwater discharge (Winter et al., 1998), rather than that driven by valley topography local to the river. Hyporheic exchange in the lower Quashnet River system is superimposed on the general upward hydraulic gradient to the stream, and therefore reduced to a thin, shallow hyporheic exchange zone (e.g. < 0.1 m depth) along the thalweg by these competing pressures (Briggs et al., 2014), as has been simulated for similar stream systems (e.g. Cardenas and Wilson 2006).

## **Methods**

A combination of fish tagging and visual spawning observations, heat tracing, geophysical surveys, and focused pore-water sampling was used to investigate the interplay between the locations of preferential brook trout spawning and the local hydrogeology. For

consistency between varied methods and years of data collection, all sample locations are spatially referenced as downstream channel distance from the fish ladder river crossing at the upper end of the study reach (Figure 2).

#### *Observations regarding repeat spawning locations*

Observations regarding discrete repeat brook trout spawning locations were made opportunistically as part of an ongoing PIT (Passive Integrated Transponder) tagging study of the native reproducing population of the Quashnet River. Large-scale trout movements are continuously monitored in the lower Quashnet River at 3 stationary fish counting sites (Figure 2a). However the spatial resolution of these counting sites, separated by hundreds of meters, is not adequate to study how brook trout utilize specific decimeter- to meter-scale groundwater discharge zones. For this finer scale characterization, dropped fish tags have also been located through roving surveys using a handheld portable PIT antenna (Biomark, Inc.) conducted in spring and fall since 2007. The dropout of PIT tags from the fish body is a process that is more likely to happen during spawning behavior in salmonids (Meyer et al 2011), so dropped tags were located electronically and spatially mapped to reveal discrete zones of repeat spawning. Although these roving surveys do not yield the temporal continuity the instream counting gates, clustering of dropped tags can be mapped at the sub-meter scale, presumably directly at trout redds. In addition, spawning brook trout were located visually during annual fall data collection events by Massachusetts Fish and Wildlife Staff, with redd development behavior captured within one seepage feature by underwater video in 2015 using a GoPro Hero camera (San Mateo, CA). We refer to the 3 most prominent sites of brook trout spawning within the study reach as Spawn 1 (113 m), Spawn 2 (146 m), and Spawn 3 (2062 m), from upstream to downstream, respectively (Figure 2).

#### *Spatial mapping of preferential groundwater discharges*

To augment existing streambed interface thermal surveys for preferential groundwater discharge (e.g. Rosenberry et al., 2016; Figure 1) and the bank-dependence of discharge location, ruggedized fiber-optic cables suitable for stream use were deployed in the river along the base of each bank from 1700 to 2160 m on June 10 through June 12, 2016 (Figure 2a). Two separate cables weighted with stainless steel armoring were installed directly along the foot of each bank on top of the streambed interface. Single-ended measurements made at the 1.01 m linear spatial sampling scale were integrated over 5-min intervals on each channel by an Oryx FO-DTS control unit (Sensornet Ltd.). During the same period, data were also collected along a high-resolution wrapped fiber-optic array for a dataset described in Kurylyk et al. (2017) but not shown here; this experimental setup resulted in measurements for each channel of 4 instrument channels recorded at 20-min intervals. Calibration for dynamic instrument drift was performed automatically using an approximately 30-m length of cable for each channel submerged in a continuously mixed ice-bath and monitored with an independent Oryx T-100 thermistor.

#### *Quantification of vertical groundwater discharge rates*

Once preferential discharge locations are located along the streambed with FO-DTS, actual vertical discharge rates can be assessed with a variety of methodologies (Kalbus et al., 2006). Temporal patterns in groundwater discharge flux rate can indicate source flowpath hydrodynamics, and be derived from bed temperature time series using vertical temperature signal transport characteristics, as reviewed by Rau et al., (2013). Custom “1DTempProfilers” designed specifically for the quantification of groundwater discharge (Briggs et al., 2014) were used to monitor streambed temperature over time along a shallow vertical profile. Profilers were deployed within a subset of the thermal anomalies previously identified with FO-DTS. The

profiler deployment locations were chosen to represent a range of preferential groundwater discharge rates/characteristics based on the on the observed FO-DTS temperature anomalies, e.g. anomalies of varied mean temperature and buffering effect (Figure 1). These preferential groundwater discharges were located: 330, 880, 1045, 1070, 1410, 1470, and 2060 m approximate downstream distance from the fish ladder crossing. These groundwater discharge locations are referred to with the prefix “GW” followed by the meter mark for the remainder of the manuscript, such that major streambed seep 330 m downstream of the fish ladder is referred to as “GW330”. Data were collected at various locations from June 11 to July 13 in 2014; August 21 to September 13 in 2015; and June 5 to July 9 in 2016. These deployments included installation of 1DTempProfilers at the nearbank and channel sides of observed repeat spawning zones.

Individual thermal data loggers (iButton Thermochron DS1922L, Maxim Integrated) were waterproofed with silicone caulking and inserted horizontally into short slotted-steel pipes (0.025 m diameter). The shallow thermal profilers were driven vertically into the streambed so that sensors were positioned at some combination of 0.01, 0.04, 0.07, and 0.11 m depths. Data were collected at temporal intervals of 0.5 hr in 2014, 2015, and 1 hr in 2016. Rosenberry et al. (2016a) found that when a subset of the 2014 streambed temperature data presented here were analyzed using the diurnal signal amplitude attenuation models employed by VFLUX2 (Irvine et al., 2015), a near 1:1 relation was found in comparison to physical seepage meter measurements of groundwater discharge ranging from 0.5 to 3  $\text{m}^3\text{d}^{-1}$ . A similar diurnal signal-based in-situ streambed thermal parameter estimation is used here.

#### *Streambed groundwater discharge and spawning zone pore water characterization*

Subsurface water samples were collected for chemical analysis at 7 major open valley

seepage locations and 3 repeat spawn locations. Geochemical data collection occurred in 2014 and 2016 along with the 1DTempProfiler deployments, while stable water isotope data were collection in August 2017. For geochemical sampling, 0.0095 m (nominal) stainless steel drivepoints were inserted to depths of 0.3, 0.6, and/or 0.9 m and Masterflex Norprenetubing was attached to the drivepoint. A peristaltic pump was used to extract pore water samples until free of obvious turbidity (typically requiring 3 min of pumping) after which the pumping rate was slowed and, the groundwater samples were collected by pumping into 60-mL HDPE syringe barrels. First an unfiltered sample for specific conductivity was pushed from the syringe into a 30-mL HDPE Nalgene sample bottle. Second, a filtered sample for anion analysis was collected after attaching a 0.2- $\mu$ m pore size (25-mm diameter) Pall polyethersulfone filter to the syringe. Lastly, the pumping rate was slowed again and an overflow cup was attached to the norprene sample tubing and held upright until overflowing, at which point DO was measured by a field colorimetric test using the manufacturer's evacuated reagent vials (Chemetrics V-2000). DO concentrations were read twice and the test repeated using an alternative vial kit if results were near the concentration range limit or out of range. The collected samples were kept cool and out of the light and analyzed for  $\text{Cl}^-$  upon return to the laboratory using standard ion chromatographic techniques.

In addition to the drivepoint samples, pore water were also collected in June 2016 from shallow depths 0.015, 0.04, 0.08 and 0.15 m below the streambed surface at locations GW1045 and Spawn 1, 2, 3 using MINIPPOINT samplers (e.g. Harvey and Fuller 1998). Water was pumped simultaneously from all depths using a multi-head pump that withdrew small-volume samples (15 mL) at low flow rates ( $1.5 \text{ mL min}^{-1}$ ) to minimize disturbance of natural subsurface fluxes and chemical gradients. Pumped lines terminated at press-on luer fittings that were

pushed onto 0.2- $\mu$ m pore size (25-mm diameter) Pall polyethersulfone filters. Samples for specific conductivity were collected whereas filtered samples were collected for anions in prelabeled 20-mL LDPE plastic scintillation vials with Polyseal<sup>TM</sup> caps. Sample lines were then attached to overflow cups and dissolved oxygen concentrations were measured as described above.

During a follow-up field effort in August, 2017 streambed pore water samples were collected at the Spawn sites and at GW1045, GW1140 (approximately 70 m downstream of GW1070), and GW1470. Additionally, two large hillslope springs were identified along the edge of the riparian zone, upstream of Spawn 1, using a handheld infrared camera (FLIR T640, FLIR Systems, Inc.). These exposed springs were sampled to identify a localized hillslope groundwater signature that would not be impacted by valley-floor peat deposits. Samples were drawn from push-point piezometers installed from 0.2-0.44 m below the sediment interface, with deeper samples collected in the hillslope springs to avoid surface organic material. Pore water was evaluated for SpC, DO, and stable water isotopes. Isotope samples were analyzed by the U.S. Geological Survey Stable Isotope Laboratory using dual-inlet isotope-ratio mass spectrometry. A substantial fraction of regional Cape Cod shallow groundwater exchanges with the numerous groundwater flow through lakes as it discharges to the coast (Walter and Masterson, 2002). It is therefore assumed that the regional Cape Cod groundwater isotopic signature is likely to indicate evaporative processes (Leblanc et al., 2008), offering a contrasting signal from locally-recharged hillslope groundwaters (no substantial evaporation). Local deuterium excess of contemporary waters can indicate groundwater that has been influenced by evaporation in lakes, and is therefore in disequilibrium with local meteoric waters. Deuterium excess was determined here as:  $d\text{-xs} = \delta^2\text{H} - 8 * \delta^{18}\text{O}$  (Dansgaard, 1964).

As mentioned previously, historic cranberry farming practices extensively modified the Quashnet River valley including the incision of drainage ditches into the floodplain. Some ditches extend from the valley wall to the main channel, whereas others are shorter or cut at angles. In addition to characterization of pore water, 34 major drainage ditches (observed flowing water) and a stream thalweg profile were spot checked for specific conductivity on June, 16 2014 using the SmarTroll probe (YSI). At a subset of these ditch locations, filtered grab samples were collected and analyzed in the laboratory for  $\text{Cl}^-$  in a similar manner as for the mini and drivepoint samples described above. In June 2016, the dataset was augmented for 5 ditch confluence locations upstream of Spawn 1.

#### *Visualizing streambed sediment geologic structure*

Ground penetrating radar (GPR) has been successfully applied to several surface water/groundwater exchange studies to characterize underlying peat and sandy deposits (e.g. Lowry et al., 2009; Comas et al., 2011) due to strong expected differences in matrix porosity (water content), which can exceed 70% in peat (Rezanezhad et al., 2016). An upstream to downstream GPR profile was collected on July 7, 2016 using a MALA HDR GX160 shielded antenna (MALA GPR, Sweden) hand-towed down the stream center channel with a small inflatable watercraft. The locations of major seep and spawning sites were specifically marked on the digital GPR record during data collection. The GPR data were processed using Reflexw software (Sandmeier, Germany) to convert reflection time to interface depth.

## **Results**

The hydrogeochemical characterization of observed, repeat trout spawning zones and other major streambed groundwater discharge zones are contrasted below. Observations



regarding repeat spawning locations.

*Observations regarding repeat spawning locations*

Out of the dozens of preferential groundwater discharge zones geolocated along the Quashnet River in this and previous work (e.g. Figure 1), brook trout appear to consistently utilize only three discrete streambed locations for repeat spawning activity. These locations coincide with steep cut banks where the river channel approaches the sand and gravel valley wall (Figure 2b,c). Specifically, trout were found to occupy small “scalloped” alcove bank features (Figure 3a) that may be formed by groundwater sapping and subsequent slumping of sandy bank materials. In winter 2016, fresh slumping and direct seepage from the newly exposed sand wall was observed at Spawn 3 (Figure 3c); a larger slump event had filled approximately 1/3 of the scalloped alcove at Spawn 2 by June 2016. Brook trout were observed clustered along the inner bank area at the Spawn 1 location in fall 2015 (Figure 3d), and this spawning behavior was captured using underwater video (Supplemental Video S1).

Dropout PIT tags have been found repeatedly in each of the 3 preferential spawn zones. Seven dropout PIT tags were located in the Spawn 3 zone in March 2017, by far the most dropped tags found in any one location since the tracking program began in 2007. The only other obvious scalloped bank features along the 2 km study reach are located at GW1045 (Figure 3b). Compared to the trout spawning zone alcoves along the valley wall cutbanks (e.g. Figure 3a), this open valley seepage alcove was overgrown with watercress and thick (tens of centimeters) loose deposits of organic material.

*Spatial mapping of preferential groundwater discharges*

As shown in Figure 1, previously collected FO-DTS data was used to guide data

collection at a subset of representative preferential streambed groundwater discharges. Additionally, paired FO-DTS cables were deployed at the base of both stream banks through a lower reach section in 2016 (Figure 2c), revealing differing thermal anomaly patterns (Figure 4; Briggs et al., 2018c). The cable along the downstream-right bank captures a large, 8-m-long cooler zone at Spawn 3 (Figure 4b), and this seepage signature is spatially reduced but visible along the opposing bank (Figure 4a). Other thermal anomalies observed along one bank show little or no signature along the other. Air temperature dropped noticeably over the final 1.5 d of deployment, and smaller cool anomalies that appeared on warm days are no longer captured by the streambed FO-DTS deployment, but the Spawn 3 signature is still visible along both cables.

#### *Quantification of vertical groundwater discharge rates*

Ambient streambed temperature signal data can be used to measure streambed thermal conduction parameters (Luce et al., 2013), which is particularly important when applying heat-based methods to quantify upward vertical fluid flux (Rosenberry et al., 2016), compared to downward fluid flux models that generally show less sensitivity to streambed thermal parameters. Diurnal signal-based thermal diffusivity measurements derived from a pair of 1DTempProfilers inserted in sandy channel sediments for a month in 2014 have the same geometric mean value of  $0.11 \text{ m}^2\text{d}^{-1}$  (Briggs et al., 2018c), and this value is used here to model vertical groundwater discharge for all locations and data collection periods (Briggs et al., 2018c). Sub-daily groundwater discharge fluxes evaluated over similar spring/early summer time periods in 2014 and 2016 show relatively stable patterns at open valley seepage zones, generally  $<1 \text{ md}^{-1}$  (Figure 6). At Spawn 1 and 3 seepage is stronger (2 to  $3.5 \text{ md}^{-1}$ ) and more variable than at open valley zones. The Darcy-based horizontal seepage estimate through the Spawn 3 bank, made using the bank piezometer, is  $2.3 \text{ md}^{-1}$ , which is similar to the temperature-based seepage rates at the Spawn 3 interface (Figure 6), and indicates lateral discharge through the cut bank

wall from a more localized groundwater flowpath. The Spawn 2 zone shows a reduced and more stable discharge rate during summer 2016, and is likely impacted by a large bank slump into this zone that occurred during the winter of 2016, partially filling the alcove. Seepage patterns collected at Spawn 1 and 2 in late-summer 2015 show greater temporal stability, even though the stream stage at the downstream USGS gage showed substantial variation. Discharge rates along the inner bank wall of the scalloped bank spawn zones were consistently higher than at bed areas located just a few meters away toward the channel.

#### *Streambed groundwater discharge and spawning zone pore water characterization*

Based on previous characterization, the Cape Cod sand and gravel aquifer generally has high DO concentrations (9 - 11 mg/L), relatively dilute specific conductance (SpC, 62  $\mu$ S/cm), and dilute chloride concentrations ( $\text{Cl}^-$ , 9.3 mg/L) at depths ranging between 12 and 20 m (Savoie et al., 2012). The groundwater that discharges to the Quashnet River, however, is often strongly variable in all three of these parameters (Harvey et al., 2018). In June 2014, drivepoint data were primarily collected in open valley seepage zones identified with FO-DTS (Figure 1); these locations are suboxic to anoxic at 0.3 and 0.6 m streambed depths (Table 1). Highest streambed seepage DO is found at GW330 in the tighter upstream valley section (4.6 mg/L at both depths) and Spawn 3, where DO is 9.0 and 7.6 mg/L at 0.3 m and 0.6 m depths, respectively (Table 1). SpC is also variable, but lowest and similar to the regional signal at GW330 and Spawn 3. Note, SpC and  $\text{Cl}^-$  are used here to indicate aquifer flowpath hydrogeochemical properties, and not suitable spawn habitat based on chemical concentration, as their range is well within general brook trout tolerances.

Drivepoint data collected at the 0.3 m depth in June 2016, primarily around spawn zones, generally show high DO and relatively low SpC at the interior of Spawn Zones 1 and 3 near the

cut bank (Table 1). Data collected a few meters toward the main channel from these near-bank spawn locations are reduced in DO with increased SpC. The Spawn 2 data were collected at the toe of the recent large sediment slump that had partially filled the alcove, and DO data are suboxic at 0.3 m (3.9 mg/L) but more oxygen enriched at 0.9 m depth (7.2 mg/L) indicating the potential for shallow streambed respiration that removes oxygen from discharging groundwater (assuming vertical flow) in the slumped material. In contrast to the spawn zones, major open valley seepage location GW1045 is nearly anoxic at all depths with SpC similar to the 2014 stream water profile grab samples ( $n=8$ ,  $101.4 \pm 1.7 \mu\text{S/cm}$ ). Little difference was observed between near-bank and channel positions at GW1045 (both are suboxic) even though a large scalloped seepage bank feature was observed (Figure 3b).

The drainage-ditch grab samples generally show  $\text{Cl}^-$  concentrations that are lower than the average 2014 channel grab samples ( $n=10$ ,  $19 \pm 0.4 \text{ mg/L}$ ), though the 2 most upstream ditches are similar to stream water, and 2 open valley ditches are appreciably higher in  $\text{Cl}^-$  (Figure 7a). Spawn Zones 1, 2, and 3 approximate the lowest  $\text{Cl}^-$  concentrations observed in drainage ditches, and Spawn 3 has a similar concentration to the adjacent 2016 streambank piezometer in both the 2014 and 2016 data. An analogous pattern is shown in the more widespread SpC data, with many drainage ditches and all spawn zones having concentrations around  $60 \mu\text{S/cm}$ , but several ditches cluster around the stream water average or higher, particularly in the open valley area.

The shallow, discrete interval shallow pore-water samples collected with the MINIPPOINT system show that streambed SpC is appreciably lower than stream water, even at the 0.02 m depth, at all near-bank spawn zones (Figure 8a). Conversely, the shallow channel sediments at Spawn 1 and open valley seepage GW1045 approximate the stream water value for

SpC. DO is high and stable along the shallow profiles (to 0.14 m) at the interior of Spawn Zones 1 and 3, but suboxic at the Spawn 1 channel sample and Spawn 2 zones, and essentially anoxic along the bank at GW1045. Center channel pore water samples at GW1045 show moderate oxygen enrichment at 0.02 m (4.6 mg/L), which may result from hyporheic mixing, as deeper intervals along the same profile are nearly anoxic.

Underwater video collected here in the fall of 2015 indicates Quashnet River brook trout clustered tightly around an approximate 1-m<sup>2</sup> bed area in Spawn 1 (Figure 3d, Video S1), directly at the base of the sandy cut bank. During the June 2016 collection of pore-water data, drivepoints were installed precisely in this area. Chemical analysis of 0.3 m depth pore water shows a strong gradient from the near-bank Spawn 1 zone to the outer alcove area, with specific conductance rising dramatically (70.6 to 143.9  $\mu\text{S}/\text{cm}$ ) and DO falling (7.28 to 4.41 mg/L) (Table 1). Spawn 3 shows a similar pattern from near-bank toward main channel (60.4 to 82.1  $\mu\text{S}/\text{cm}$  SpC; 9.11 to 1.76 mg/L DO), and Spawn 2, although complicated by the large slump during the previous winter, shows an increase in SpC from 70.6 to 139.3  $\mu\text{S}/\text{cm}$  from the inner to outer alcove. Conversely, pore water collected at 0.3, 0.6, and 0.9 m depths in the open valley seepage alcove at GW1045 (pictured in Figure 3b) are functionally anoxic with elevated SpC compared to inner spawn zones, and little gradient from bank to channel.

Pore water data collected in August 2017 indicate that all three Spawn sites are similar to emergent hillslope springs, characterized by relatively high DO and low SpC compared to major open valley streambed seepage zones that are anoxic with higher SpC (Table 2). Additionally, the stable isotopic signatures of the hillslope and Spawn zones are similar, but contrasted by the lower deuterium excess metric determined for the open valley seepages. This indicates that groundwater discharging through the streambed away from the hillslope shows the evaporative

signature of groundwater flow through lakes, and can therefore be considered regional discharge, compared to locally recharged hillslope groundwaters apparently favored by trout for spawning..

#### *Visualizing streambed sediment geologic structure*

Radar data were collected over most of the study reach length depicted in Figure 2a, and although spatial reference data were not collected for each sample point due to integrated Global Positioning System failure, Spawn and groundwater discharge zones of interest were precisely marked in the record (Figure 5). The GPR data collected along the thalweg adjacent to Spawn 1 and 2 indicate a contiguous thin layer of material underlies the sandy streambed that may be peat deposited over deeper sands and gravels (Figure 5a). The GPR profile through open valley groundwater discharge locations GW1045 and GW1070 show the strongest radar signal reflectors of anywhere along the open valley section (Figure 5b). These discontinuous geologic structures are interpreted as layered sand, gravel, interspersed with thicker peat deposits. Otherwise, discontinuous reflections indicative of sediment type-interfaces of variable depth are observed near downstream open valley seepage zones where strongly attenuated GPR signals indicate thick lenses of buried peat with high water content (Figure 5b,c).

#### **Discussion**

Heat tracing reconnaissance technologies, such as FO-DTS and thermal infrared, offer an efficient means to comprehensively characterize a subset of preferential groundwater discharge points at the reach to watershed scale (e.g. Figure 1, Figure 4). Using the groundwater-fed Quashnet River as an example, Rosenberry et al. (2016) showed that cold streambed interface anomalies in summer indeed corresponded to discrete zones of particularly high groundwater discharge through streambed sediments. This spatial characterization of discharge points alone is not sufficient to characterize the physical and chemical drivers of niche critical cold-water

habitat, but can efficiently guide additional data collection, as was done here. Compared to more randomly distributed streambed field parameter surveys, or larger spatial scale evaluations of net groundwater discharge made with differential gaging, comprehensive spatial mapping of groundwater discharges is a great advance in the context of understanding groundwater dependent ecosystems. However, in fast flowing streams, FO-DTS cable placement on the streambed will likely impact which specific groundwater discharge zones are captured with FO-DTS, as shown here by applying cables along opposite banks through the Spawn 3 area (Figure 4). The largest seepage zones may have a spatial footprint that encompasses the streambed area from bank to bank (e.g., the Spawn 3 cold anomaly), but a subset of more discrete seepage zones are bound to be missed with a single linear cable deployment. We did not capture Spawn Zones 1 and 2 in early FO-DTS field efforts (Figure 1), but fish tracking indicated their importance to trout spawning behavior. Therefore, in studies of niche stream habitat as influenced by preferential groundwater discharge, a combination of heat tracing and biological observation may be needed to both identify major discharge points and discern which points are directly used by the biota of interest (e.g. brook trout).

In a study of the regional Cape Cod aquifer condition, Frimpter and Gay (1979) state that groundwater is typically near DO saturation, except downgradient of peat or river bottom sediments, where consumption of DO allows the mobilization of natural iron and manganese. Visible observations along the open valley section, in addition to streambed sediment coring (Briggs et al. 2014), revealed widespread coating of shallow streambed sediment grains with metal oxides, consistent with the conceptual model of organic material influence on near-surface groundwater (Figure 9). Aquifer recharge passing through upgradient groundwater flow-through kettle lakes (e.g. Stoliker *et al.* 2016) may also serve to decrease the DO content of regional

flowpaths that discharge vertically through the bed of the Quashnet River, although we hypothesize that localized peat deposits may be the primary control on both seepage zone distribution and chemistry.

Out of the dozens of preferential groundwater discharge zones located along the lower Quashnet with heat tracing, most were suboxic to anoxic (Table 1). Brook trout consistently prefer three areas for fall spawning, all along meander bend cut banks into the sand and gravel valley wall. Zones of locally enhanced seepage, likely controlled by subtle differences in sediment hydraulic conductivity, can lead to groundwater sapping of fines, reduction in bank stability, and consequent slumping of bank material into the river; this process was observed in real-time at the Spawn 3 meander in February 2016 (Figure 3c). Slumping effectively forms *seepage-driven* alcoves outside of the main flow and more suitable for redd placement, along with a more favorable coarse sand and gravel substrate (Bowerman et al., 2014; Hausle and Coble, 1976; Raleigh, 1982).

In other systems, trout have been observed to occupy microhabitat around and within groundwater discharge zones, even segregating by fish size and desirable temperature range (e.g., Figure 2.4.1.2 in Torgersen et al. 2012). Here, real-time observation and visual imagery show trout clustering tightly against the bank in Spawn 3 (Figure 3d, Video S1) where pore water was found to be more oxygen rich and lower in SpC. Month-long time series of vertical groundwater discharge rates are reduced considerably from near-bank to near-channel at all spawning zones (Figure 6), indicating in part a reduction in streambed hydraulic conductivity as influenced by peat deposits under the main channel as observed in GPR data (Figure 5). The combined evidence of higher near-bank vertical groundwater flux rates and DO, combined with lower SpC, indicates limited interaction between shallow groundwater flowpaths and peat



against the meander bend cut banks. It appears that even short travel distances through organic deposits toward the center channel at Spawn 1 and 2 may be sufficient to increase total dissolved solids and deplete DO, as observed in other systems (e.g. Levy et al., 2016), and render upwelling zones undesirable for redd construction. Therefore, near-surface channel sediments may need to be specifically characterized in preferential groundwater discharge zones, as net chemical reactivity over the last ~1 m of transport may dominate that along km of upgradient groundwater flow through mineral soils.

Only where seepage was observed to emanate directly from the valley wall sands and gravels, such as the newly exposed slump in Figure 3C, may groundwater discharge reliably support overwinter trout egg development. These features are apparently similar to the numerous cold-water alcove patches observed in another stream system by Ebersole et al. (2003). In that study of preferential salmonid habitat, alcoves were often located where streams converged on valley walls and were the most abundant type of discrete cold-water habitat type identified. Conversely, valley wall alcoves were the least-common type of seep morphology observed along the Quashnet River. It is likely that the artificial reduction in channel sinuosity along the Quashnet River by farming practices has reduced possible higher-quality spawning locations.

Other bank alcove features with strong groundwater discharge found along the open valley section (Figure 3b) were highly influenced by organic material deposition and did not apparently support spawning habitat. Our research indicates that in lowland systems with organic-rich floodplain sediments valley wall alcoves alone create favored brook trout spawning habitat via local mineral soil-dominated groundwater discharge flowpaths as shown in conceptual Figure 9. This finding might help inform future ecologically-based stream restoration practices in using the natural landscape to predict desirable preferential groundwater discharge

points, as was recently done by Hare et al., (2017) to inform the engineering of a large-scale cranberry bog restoration.

The pore-water SpC, Cl<sup>-</sup>, and DO data alone do not definitively show that seepage at the cut bank spawn sites is derived from more localized groundwater recharge, as opposed to regional groundwater that is unadulterated by buried peat lenses. However, the hydrodynamic data derived from long-term vertical temperature profiling in seepage zones does offer additional insight. In general, groundwater discharge rates are more variable at cut bank spawn zones than in the open valley streambed zones (Figure 6), and this variability may be tied to shorter-term changes in local river stage and/or water table depth, impacting the local hydraulic gradient. The relatively stable patterns of open valley groundwater discharge may be controlled by the regional gradient where the flowpath-length term dominates the Darcy relation, and is therefore relatively insensitive to local changes in river stage and water table fluctuations. Further, the stable water isotope data display evaporative signatures at the open valley streambed discharge sites, indicating regional groundwater that has passed through one or more upgradient flow-through lakes (Table 2). In contrast, the Spawn sites all show isotope signals that fall along the local meteoric water line, and therefore likely represent recharge to the hillslopes more local to the river. These localized groundwater flow systems would be expected to be less-influenced by regional groundwater contamination, which is widespread in the regional Cape Cod aquifer (Walter and Masterson, 2002).

Groundwater drainage-ditch data collected along the river corridor indicate low SpC/Cl<sup>-</sup> conditions exist for the majority of ditches throughout the lower Quashnet River riparian areas (Figure 7). The hillslope piezometer in sand and gravel at the down valley wall has a similar chemical signature along with high DO. This similarity is further indication that low-SpC

groundwater discharges even to the lower portion of the river corridor, but is predominantly modified chemically by travel through near-stream organics. The relic drainage ditches allow discharging groundwater to effectively short circuit the valley floor peat deposits and remain high in DO, similar to the natural valley wall springs and cut bank alcoves. Future restoration strategies that seek to actively enhance groundwater discharge (e.g. Kurylyk et al., 2015a) may consider capitalizing on this short circuit behavior, possibly by auguring through buried streambed peat or movement of the stream channel toward the valley wall to create more desirable brook trout aquatic habitat.

## **Conclusions**

The three repeatedly utilized discrete spawning zone locations that have been identified over 10 yr+ of observation have coupled strongly discharging groundwater with high DO concentration. A conceptual diagram of the hydrogeochemical setting of spawn zones vs other non-favored streambed groundwater discharge locations is shown in Figure 9. Spawn zones are located exclusively in side alcoves of the channel created by bank slumps along meanders where the river cuts into steep hillslopes along the glacial sands and gravel valley wall. In the alcoves at the base of the cut banks, hillslope groundwater with high DO concentration is discharged through the streambed without appreciable loss of oxygen. Just a few meters away toward the main channel, however, groundwater consistently discharges at lower rates, is reduced in DO, and increased in SpC. The lowest oxygen concentrations in groundwater are associated with water emerging from the streambed adjacent to wide riparian areas that flank the Quashnet in the open valley section of the study reach, even though groundwater discharge rates were also relatively high. In the open valley, where the stream is not near the valley walls, proximity to the stream bank does not seem to control seepage chemistry, and GPR data indicated thick zones of

discontinuous streambed peat. In this and other groundwater-dominated streams that are expected to serve as climate refugia for future native trout populations, hyporheic exchange will be limited by strong upward hydraulic gradient. Therefore, preferential spawning habitat in such lowland valley systems may be primarily supported by discrete zones of oxic groundwater upwelling at the meter to sub-meter scale as has been indicated by previous work (e.g. Curry et al., 1995).

In systems where all groundwater discharge is universally anoxic, preferential salmonid spawning zonation may be controlled by points of downwelling hyporheic water where shallow sediments remain high in DO (Buffington and Tonina, 2009; Cardenas et al., 2016). However, these hyporheic areas will deliver cold surface water to shallow sediments during winter, which may impair overwintering brook trout eggs (French et al., 2016). Here, and in many other coastal systems, groundwater temperature is expected to range approximately 10-12 °C, which is an ideal range for brook trout egg development (Raleigh, 1982). Points of oxic groundwater upwelling devoid of near-stream buried organics, combined with a recirculating side alcove and favorable sand and gravel sediments, may provide ideal and unique groundwater seepage-enabled preferential spawning habitat for native trout.

Stream surface or streambed interface heat tracing of groundwater discharge offers an efficient means to locate discrete seepage zones, but offers only limited insight into source groundwater flowpath hydraulics and geochemistry. A combined toolkit that also includes spatially-informed (using heat tracing) geochemical and isotope sampling and geophysical imaging can be used to trace groundwater flowpaths back into the source aquifer, and develop a robust hydrogeochemical characterization. Additionally, as digital elevation models become more refined and combined with infrared data derived from Unmanned Aircraft Systems, remote

identification of relatively small features such as the seepage alcoves described here should be possible. Comprehensive and process-based characterization niche stream habitat can be used to guide stream ecological restoration design that directly incorporates the local preferential groundwater discharge template.

## **Acknowledgements**

Comments from anonymous reviewers and U.S. Geological Survey (USGS) reviews by Nathaniel Hitt and Paul Barlow are gratefully acknowledged. The U.S. Environmental Protection Agency (USEPA) through its Office of Research and Development partially funded and collaborated in the research described here under agreement number DW-14-92381701 to the USGS. The USGS authors were supported by the following USGS entities: Office of Groundwater, Water Availability and Use Science Program, National Water Quality Program, and the Toxics Substances Hydrology Program. Field and laboratory assistance from Allison Swartz, Jay Choi, Jenny Lewis, Yao Du, Danielle Hare, Courtney Scruggs, Rayna Mitzman, David Rey, Geoff Delin, Eric White, MassWildlife Southeast District Staff, Jennifer Salas, and volunteers from Trout Unlimited is greatly appreciated. The manuscript has been subjected to Agency review and approved for publication. The views expressed in this article are those of the authors and do not necessarily represent the views or policies of the USEPA. Any use of trade, firm, or product names is for descriptive purposes only and does not imply endorsement by the U.S. Government.

654 **References**

- 655 Annett, B., Gerlach, G., King, T. L. and Whiteley, A. R.: Conservation Genetics of Remnant  
656 Coastal Brook Trout Populations at the Southern Limit of Their Distribution: Population  
657 Structure and Effects of Stocking, *Trans. Am. Fish. Soc.*, 141(5), 1399–1410,  
658 doi:10.1080/00028487.2012.694831, 2012.
- 659 Back, W., Baedeker, M. J. and Wood, W. W.: Scales in hydrogeology: a historical perspective, in  
660 *Regional Water Quality*, pp. 11–128, Van Nostrand Reinhold, New York., 1993.
- 661 Baird, O. E. and Krueger, C. C.: Behavioral thermoregulation of brook and rainbow trout:  
662 comparison of summer habitat use in an Adirondack River, New York, *Trans. Am. Fish. Soc.*,  
663 132, 1194–1206, 2003.
- 664 Barlow, P. M. and Hess, K. M.: Simulated Hydrologic Responses of the Quashnet River Stream-  
665 Aquifer System to Proposed Ground-Water Withdrawals, Cape Cod, Massachusetts, U.S. Geol.  
666 *Surv. Rep.* 93-4064, 51, 1993.
- 667 Bowerman, T., Neilson, B. T. and Budy, P.: Effects of fine sediment, hyporheic flow, and  
668 spawning site characteristics on survival and development of bull trout embryos, *Can. J. Fish.*  
669 *Aquat. Sci.*, 71, 1059–1071, 2014.
- 670 Briggs, M. A., Lautz, L. K., Buckley, S. F. and Lane, J. W.: Practical limitations on the use of  
671 diurnal temperature signals to quantify groundwater upwelling, *J. Hydrol.*, 519, 1739–1751,  
672 doi:10.1016/j.jhydrol.2014.09.030, 2014.
- 673 Briggs, M. A., Hare, D. K., Boutt, D. F., Davenport, G. and Lane, J. W.: Thermal infrared video  
674 details multiscale groundwater discharge to surface-water through macropores and peat pipes,  
675 *Hydrol. Process. HPEye*, 30(14), 2510–2511, doi:10.1002/hyp.10722, 2016.
- 676 Briggs, M. A., White, E. A. and Lane, J. W.: Surface geophysical data for study of preferential  
677 brook trout spawning habitat, Cape Cod, USA: U.S. Geological Survey data release, ,  
678 doi:https://doi.org/10.5066/F7PN93QF, 2017.
- 679 Briggs, M. A., Johnson, Z. C., Snyder, C. D., Hitt, N. P., Kurylyk, B. L., Lautz, L., Irvine, D. J.,  
680 Hurley, S. T. and Lane, J. W.: Inferring watershed hydraulics and cold-water habitat persistence  
681 using multi-year air and stream temperature signals, *Sci. Total Environ.*, 636, 1117–1127,  
682 doi:10.1016/j.scitotenv.2018.04.344, 2018a.
- 683 Briggs, M. A., Lane, J. W., Snyder, C. D., White, E. A., Johnson, Z. C., Nelms, D. L. and Hitt,  
684 N. P.: Shallow bedrock limits groundwater seepage-based headwater climate refugia,  
685 *Limnologica*, 68, 142–156, doi:10.1016/j.limno.2017.02.005, 2018b.
- 686 Briggs, M. A., Scruggs, C. R., Hurley, S. T. and White, E. A.: Temperature and geophysical data  
687 collected along the Quashnet River, Mashpee/Falmouth MA: U.S. Geological Survey data  
688 release, , doi:10.5066/F7PN93QF, 2018c.
- 689 Buffington, J. M. and Tonina, D.: A three-dimensional model for analyzing the effects of salmon  
690 redds on hyporheic exchange and egg pocket habitat A three-dimensional model for analyzing

691 the effects of salmon redds on hyporheic exchange and egg pocket habitat, *Can. J. Fish. Aquat.*  
692 *Sci.*, 66, 2157–2173, doi:10.1139/F09-146, 2009.

693 Burns, E. R., Zhu, Y., Zhan, H., Manga, M., Williams, C. F., Ingebritsen, S. E. and Dunham, J.:  
694 Thermal effect of climate change on groundwater-fed ecosystems, *Water Resour. Res.*, 53,  
695 3341–3351, doi:10.1002/2016WR020007, 2017.

696 Cardenas, M. B. and Wilson, J. L.: The influence of ambient groundwater discharge on exchange  
697 zones induced by current-bedform interactions, *J. Hydrol.*, 331(1–2), 103–109, 2006.

698 Cardenas, M. B., Ford, A. E., Kaufman, M. H., Kessler, A. J. and Cook, P. L. M.: Hyporheic  
699 flow and dissolved oxygen distribution in fish nests: the effects of open channel velocity,  
700 permeability patterns, and groundwater upwelling, *J. Geophys. Res. Biogeosciences*, 121, 3113–  
701 3130, doi:10.1002/2016JG003381, 2016.

702 Comas, X., Slater, L. and Reeve, A. S.: Pool patterning in a northern peatland: Geophysical  
703 evidence for the role of postglacial landforms, *J. Hydrol.*, 399(3–4), 173–184,  
704 doi:10.1016/j.jhydrol.2010.12.031, 2011.

705 Crisp: A desk study of the relationship between temperature and hatching time for the eggs of  
706 five species of salmonid species, *Freshw. Biol.*, 11(4), 361–368, doi:10.1111/j.1365-  
707 2427.1981.tb01267.x, 1981.

708 Cunjak, R. A. and Power, G.: Seasonal changes in the physiology of brook trout, *Salvelinus*  
709 *fontinalis* (Mitchill), in a sub-Arctic river system, *J. Fish Biol.*, 29, 279–288, 1986.

710 Curry, R., Noakes, D. L. G. and Morgan, G. E.: Groundwater and the incubation and emergence  
711 of brook trout ( *Salvelinus fontinalis* ), *Can. J. Fish. Aquat. Sci.*, 52, 1741–1749, 1995.

712 Dansgaard, W.: Stable isotopes in precipitation, *Tellus*, 16(4), 436–468,  
713 doi:10.3402/tellusa.v16i4.8993, 1964.

714 Dugdale, S. J.: A practitioner’s guide to thermal infrared remote sensing of rivers and streams:  
715 recent advances, precautions and considerations, *WIREs Water*, doi:10.1002/wat2.1135, 2016.

716 Dugdale, S. J., Bergeron, N. E. and St-Hilaire, A.: Spatial distribution of thermal refuges  
717 analysed in relation to riverscape hydromorphology using airborne thermal infrared imagery,  
718 *Remote Sens. Environ.*, 160, 43–55, doi:10.1016/j.rse.2014.12.021, 2015.

719 Ebersole, J. L., Liss, W. J. and Frissell, C. A.: Cold water patches in warm streams:  
720 physicochemical characteristics and the influence of shading, *J. Am. Water Resour. Assoc.*,  
721 59860, 355–368, 2003.

722 French, W. E., Vondracek, B., Ferrington, L. C., Finlay, J. C. and Dieterman, D. J.: Brown trout  
723 (*Salmo trutta*) growth and condition along a winter thermal gradient in temperate streams, *Can. J.*  
724 *Fish. Aquat. Sci.*, 9(June), 1–9, doi:10.1139/cjfas-2016-0005, 2016.

725 Frimpter, M. H. and Gay, F. B.: Chemical quality of ground water on Cape Cod, Massachusetts,  
726 *Water-Resources Investig. Rep.* 79-65, 1979.

727 Geist, D. R., Hanrahan, T. P., Arntzen, E. V., McMichael, G. A., Murray, C. J. and Chien, Y.:  
 728 Physicochemical Characteristics of the Hyporheic Zone Affect Redd Site Selection by Chum  
 729 Salmon and Fall Chinook Salmon in the Columbia River, North Am. J. Fish. Manag., 22, 1077–  
 730 1085, 2002.

731 Grinsven, M. Van, Mayer, A. and Huckins, C.: Estimation of Streambed Groundwater Fluxes  
 732 Associated with Coaster Brook Trout Spawning Habitat, , 50(3), 432–441, doi:10.1111/j.1745-  
 733 6584.2011.00856.x, 2012.

734 Hare, D. K., Briggs, M. A., Rosenberry, D. O., Boutt, D. F. and Lane, J. W.: A comparison of  
 735 thermal infrared to fiber-optic distributed temperature sensing for evaluation of groundwater  
 736 discharge to surface water, J. Hydrol., 530, 153–166, doi:10.1016/j.jhydrol.2015.09.059, 2015.

737 Hare, D. K., Boutt, D. F., Clement, W. P., Hatch, C. E., Davenport, G. and Hackman, A.:  
 738 Hydrogeological controls on spatial patterns of groundwater discharge in peatlands, Hydrol.  
 739 Earth Syst. Sci., (21), 6031–6048, doi:10.5194/hess-2017-282, 2017.

740 Harvey, J. W. and Fuller, C. C.: Effect of enhanced manganese oxidation in the hyporheic zone  
 741 on basin-scale geochemical mass balance, , 34(4), 623–636, 1998.

742 Harvey, J. W., Briggs, M. A., Buskirk, B., Swartz, A., Lewis, J. and Du, Y.: Surface water and  
 743 groundwater water chemistry data collected along the Quashnet River, Mashpee/Falmouth, MA:  
 744 U.S. Geological Survey data release, , doi:10.5066/F7M044MF, 2018.

745 Hausle, D. A. and Coble, D. W.: Influence of sand in redds on survival and emergence of brook  
 746 trout (*Salvelinus fontinalis*), Trans. Am. Fish. Soc., 105(1), 57–63, 1976.

747 Hitt, N. P., Snook, E. L. and Massie, D. L.: Brook trout use of thermal refugia and foraging  
 748 habitat influenced by brown trout, Can. J. Fish. Aquat. Sci., 74(3), 406–418, doi:10.1139/cjfas-  
 749 2016-0255, 2017.

750 Hudy, M., Thieling, T. M., Gillespie, N. and Smith, E. P.: Distribution, status, and land use  
 751 characteristics of subwatersheds within the native range of brook trout in the Eastern United  
 752 States, North Am. J. Fish. Manag., 28(4), 1069–1085, 2008.

753 Irvine, D. J., Lautz, L. K., Briggs, M. A., Gordon, R. P. and McKenzie, J. M.: Experimental  
 754 evaluation of the applicability of phase, amplitude, and combined methods to determine water  
 755 flux and thermal diffusivity from temperature time series using VFLUX 2, J. Hydrol., 531, 728–  
 756 737, 2015.

757 Isaak, D. J., Young, M. K., Nagel, D. E., Horan, D. L. and Groce, M. C.: The cold-water climate  
 758 shield: Delineating refugia for preserving salmonid fishes through the 21st century, Glob. Chang.  
 759 Biol., 21(7), 2540–2553, doi:10.1111/gcb.12879, 2015.

760 Kalbus, E., Reinstorf, F. and Schirmer, M.: Measuring methods for groundwater-surface water  
 761 interactions: a review, Hydrol. Earth Syst. Sci., 10, 873–887, 2006.

762 Krause, S., Tecklenburg, C., Munz, M. and Naden, E.: Streambed nitrogen cycling beyond the  
 763 hyporheic zone: Flow controls on horizontal patterns and depth distribution of nitrate and  
 764 dissolved oxygen in the upwelling groundwater of a lowland river, J. Geophys. Res.



765 Biogeosciences, 118(1), 54–67, doi:10.1029/2012JG002122, 2013.

766 Kurylyk, B. L., MacQuarrie, K. T. B., Linnansaari, T., Cunjak, R. A. and Curry, R. A.:  
 767 Preserving , augmenting , and creating cold-water thermal refugia in rivers : concepts derived  
 768 from research on the Miramichi River , New Brunswick ( Canada ), Ecohydrology,  
 769 1108(October 2014), 1095–1108, doi:10.1002/eco.1566, 2015a.

770 Kurylyk, B. L., MacQuarrie, K. T. B., Caissie, D. and McKenzie, J. M.: Shallow groundwater  
 771 thermal sensitivity to climate change and land cover disturbances: Derivation of analytical  
 772 expressions and implications for stream temperature modeling, Hydrol. Earth Syst. Sci., 19(5),  
 773 2469–2489, doi:10.5194/hess-19-2469-2015, 2015b.

774 Kurylyk, B. L., Irvine, D. J., Carrey, S., Briggs, M. A., Werkema, D. and Bonham, M.: Heat as a  
 775 hydrologic tracer in shallow and deep heterogeneous media: analytical solution, spreadsheet tool,  
 776 and field applications, Hydrol. Process., 31(14), 2648–2661, doi:10.1002/hyp.11216, 2017.

777 Leblanc, B. D. R., Massey, A. J., Cochrane, J. J., King, J. H., Smith, K. P. and Survey, U. S. G.:  
 778 Distribution and Migration of Ordnance- Related Compounds and Oxygen and Hydrogen Stable  
 779 Isotopes in Ground Water near Snake Pond , Sandwich , Massachusetts , 2001 – 2006, Scientific  
 780 Investigations Report 2008–5052, , 2001–2006, 2008.

781 LeBlanc, D. R., Guswa, J. H., Frimpter, M. H. and Londquist, C. J.: Ground-water resources of  
 782 Cape Cod, Massachusetts: U.S. Geological Survey Investigations Atlas HA-692, 4 sheets, 1986.

783 Levy, Z. F., Siegel, D. I., Glaser, P. H., Samson, S. D. and Dasgupta, S. S.: Peat porewaters have  
 784 contrasting geochemical fingerprints for groundwater recharge and discharge due to matrix  
 785 diffusion in a large, northern bog-fen complex, J. Hydrol., 541, 941–951,  
 786 doi:10.1016/j.jhydrol.2016.08.001, 2016.

787 Lowry, C. S., Fratta, D. and Anderson, M. P.: Ground penetrating radar and spring formation in a  
 788 groundwater dominated peat wetland, J. Hydrol., 373(1–2), 68–79,  
 789 doi:10.1016/j.jhydrol.2009.04.023, 2009.

790 Luce, C. H., Tonina, D., Gariglio, F. and Applebee, R.: Solutions for the diurnally forced  
 791 advection-diffusion equation to estimate bulk fluid velocity and diffusivity in streambeds from  
 792 temperature time series, Water Resour. Res., 49(1), 488–506, doi:10.1029/2012WR012380,  
 793 2013.

794 MacCrimmon, H. R. and Campbell, S. C.: World Distribution of Brook Trout, *Salvelinus*  
 795 *fontinalis*, J. Fish. Res. Board Canada, 26(1699–1725), 1969.

796 Mathews, K. R. and Berg, N. H.: Rainbow trout responses to water temperature and dissolved  
 797 oxygen stress in two southern California stream pools, J. Fish Biol., 59, 50–67, 1997.

798 Modica, E.: Source and age of ground-water seepage to streams, USGS Fact Sheet Fact Sheet  
 799 063-99, 1999.

800 Montgomery, D. R., Buffington, J. M., Peterson, N. P., SchuettHames, D. and Quinn, T. P.:  
 801 Stream-bed scour, egg burial depths, and the influence of salmonid spawning on bed surface  
 802 mobility and embryo survival, Can. J. Fish. Aquat. Sci., 53(5), 1061–1070, doi:10.1139/cjfas-53-

803 5-1061, 1996.

804 Mullan, J. W.: The sea run or “Salter” brook trout (*Salvelinus fontinalis*) fishery of the coastal  
805 streams of Cape Cod, Massachusetts, Massachusetts Div. Fish. Game, Bull. 17, 1958.

806 Obruca, W. and Hauer, C.: Physical laboratory analyses of intergravel flow through brown trout  
807 redds ( *Salmo trutta fario* ) in response to coarse sand infiltration, Earth Surf. Process.  
808 Landforms, doi:10.1002/esp.4009, 2016.

809 Petty, J. T., Hansbarger, J. L., Huntsman, B. M. and Mazik, P. M.: Transactions of the American  
810 Fisheries Society Brook Trout Movement in Response to Temperature , Flow , and Thermal  
811 Refugia within a Complex Appalachian Riverscape Brook Trout Movement in Response to  
812 Temperature , Flow , and Thermal Refugia within a Compl, Trans. Am. Fish. Soc., 141(4),  
813 1060–1073, doi:10.1080/00028487.2012.681102, 2012.

814 Raleigh, R. F.: Habitat suitability index models: Brook trout., U.S. Dept. Int., Fish Wildl. Serv.,  
815 FWS/OBS-82, 1–42, 1982.

816 Rau, G. C., Andersen, M. S., McCallum, A. M., Roshan, H. and Acworth, R. I.: Heat as a tracer  
817 to quantify water flow in near-surface sediments, Earth-Science Rev., 129, 40–58,  
818 doi:10.1016/j.earscirev.2013.10.015, 2014.

819 Rezanezhad, F., Price, J. S., Quinton, W. L., Lennartz, B., Milojevic, T. and Cappellen, P. Van:  
820 Structure of peat soils and implications for water storage , fl ow and solute transport : A review  
821 update for geochemists, Chem. Geol., 429, 75–84, doi:10.1016/j.chemgeo.2016.03.010, 2016.

822 Rosenberry, D. O., Briggs, M. A., Delin, G. and Hare, D. K.: Combined use of thermal methods  
823 and seepage meters to efficiently locate, quantify, and monitor focused groundwater discharge to  
824 a sand-bed stream, Water Resour. Res., 52, 4486–4503, doi:10.1002/2016WR018808, 2016.

825 Seitzinger, S., Harrison, J. a, Böhlke, J. K., Bouwman, a F., Lowrance, R., Peterson, B., Tobias,  
826 C. and Van Drecht, G.: Denitrification across landscapes and waterscapes: a synthesis., Ecol.  
827 Appl., 16(6), 2064–90 [online] Available from: <http://www.ncbi.nlm.nih.gov/pubmed/17205890>,  
828 2006.

829 Snook, E. L., Letcher, B. H., Dubreuil, T. L., Zydlewski, J., Donnell, M. J. O., Whiteley, A. R.,  
830 Hurley, S. T. and Danylchuk, A. J.: Movement patterns of Brook Trout in a restored coastal  
831 stream system in southern Massachusetts, Ecol. Freshw. Fish, 26, 360–375,  
832 doi:10.1111/eff.12216, 2016.

833 Steel, E. A., Beechie, T. J., Torgersen, C. E. and Fullerton, A. H.: Envisioning, Quantifying, and  
834 Managing Thermal Regimes on River Networks, Bioscience, 67(6), 506–522,  
835 doi:10.1093/biosci/bix047, 2017.

836 Stoliker, D. L., Repert, D. A., Smith, R. L., Song, B., Leblanc, D. R., Mccobb, T. D., Conaway,  
837 C. H., Hyun, S. P., Koh, D., Moon, H. S. and Kent, D. B.: Hydrologic Controls on Nitrogen  
838 Cycling Processes and Functional Gene Abundance in Sediments of a Groundwater Flow-  
839 Through Lake, Environ. Sci. Technol., 50, 3649–3657, doi:10.1021/acs.est.5b06155, 2016.

840 Walter, B. D. A. and Masterson, J. P.: Simulated Pond-Aquifer Interactions under Natural and

841 Stressed Conditions near Snake Pond , Cape Cod , Water-Resources Investig. Rep. 99-4174, 34,  
842 2002.

843 Wehrly, K., Wang, L. and Mitro, M.: Field-based estimates of thermal tolerance limits for trout:  
844 incorporating exposure time and temperature fluctuation, Trans. Am. Fish. Soc., 136, 365–374,  
845 2007.

846 Winter, T. C., Harvey, J. W., Franke, O. L. and Alley, W. M.: Ground water and surface water; a  
847 single resource, Gr. Water U . S . Geol. Surv. Circ. 1139, 79, 1998.

848

849

850 **Tables**

851 Table 1. 2014 and 2016 drivepoint pore-water chemistry data collected in major streambed  
 852 groundwater discharge zones located with fiber-optic heat tracing, and in zones of observed  
 853 repeat trout spawning directly along the bank and farther toward the stream center channel.

<i>open valley groundwater discharges</i>	<i>0.3 m depth</i>		<i>0.6 m depth</i>	
	DO	SpC	DO	SpC
	mg/L	μS/cm	mg/L	μS/cm
GW330	4.6	53.8	4.6	61.3
GW880	1.4	97.7	3.4	65.1
GW1045	0.1	78.8	0.0	82.5
GW1045 (bank)	0.16	105.5	0.39	104.0
GW1045 (channel)	0.31	99.1	0.18	96.4
GW1070	0.2	100.0	0.2	89.8
GW1410	0.0	77.7	0.0	79.0
GW1470	0.1	69.1	0.0	64.3
GW2060	1.4	75.0	0.5	79.4
<b>mean</b>	<b>0.9</b>	<b>84.1</b>	<b>1.0</b>	<b>80.2</b>
<i>spawning locations (channel)</i>	<i>0.3 m depth</i>		<i>0.9 m depth</i>	
Spawn 1 channel	4.41	143.9	5.68	143.2
Spawn 2 channel	5.25	139.3	n/a	n/a
Spawn 3 channel	1.76	82.1	2.68	79.9
<b>mean</b>	<b>3.8</b>	<b>121.8</b>	<b>4.2</b>	<b>111.6</b>
<i>spawning locations (bank)</i>	<i>0.3 m depth</i>		<i>0.9 m depth</i>	
Spawn 1 bank	7.28	70.6	9.76	55.9
Spawn 2 bank	3.89	70.8	7.17	57.6
Spawn 3 bank (2016)	9.11	60.4	4.91	71.9
Spawn 3 bank (2014)	9.0	56.4	7.6 (0.6 m)	60.9 (0.6 m)
<b>mean</b>	<b>7.3</b>	<b>64.6</b>	<b>7.4</b>	<b>61.6</b>

854

855 Table 2. 2017 drivepoint pore-water chemistry and stable water isotope data collected in a subset  
856 of major streambed groundwater seepage zones, zones of observed repeat trout spawning, and  
857 from springs located above the water line along the same hillslope as the meander cutbanks of  
858 Spawn 1 and Spawn 2.

<i>location</i>	<i>sample depth</i>	<i>SpC</i>	<i>DO</i>	$\delta^2H$	$\delta^{18}O$	<i>d-xs</i>
	(m)	( $\mu\text{S/cm}$ )	(mg/L)	(‰)	(‰)	$\delta^2\text{H} - 8 * \delta^{18}\text{O}$
Hillslope 1	40	74.82	5.004	-51.38	-8.2	<b>14.22</b>
Hillslope 2	44	60.59	9.318	-51.81	-8.73	<b>18.03</b>
Spawn 1	20	72.45	6.853	-48.9	-7.9	<b>14.3</b>
Spawn 2	20	51.75	5.419	-48.2	-7.95	<b>15.4</b>
Spawn 3	20	42.62	9.054	-44.32	-7.33	<b>14.32</b>
GW1045	20	109.8	0.043	-34.03	-4.93	<b>5.41</b>
GW1140	20	103.4	0.043	-32.56	-4.8	<b>5.84</b>
GW1470	20	97.68	0.04	-33.05	-4.72	<b>4.71</b>

859

## Figure List

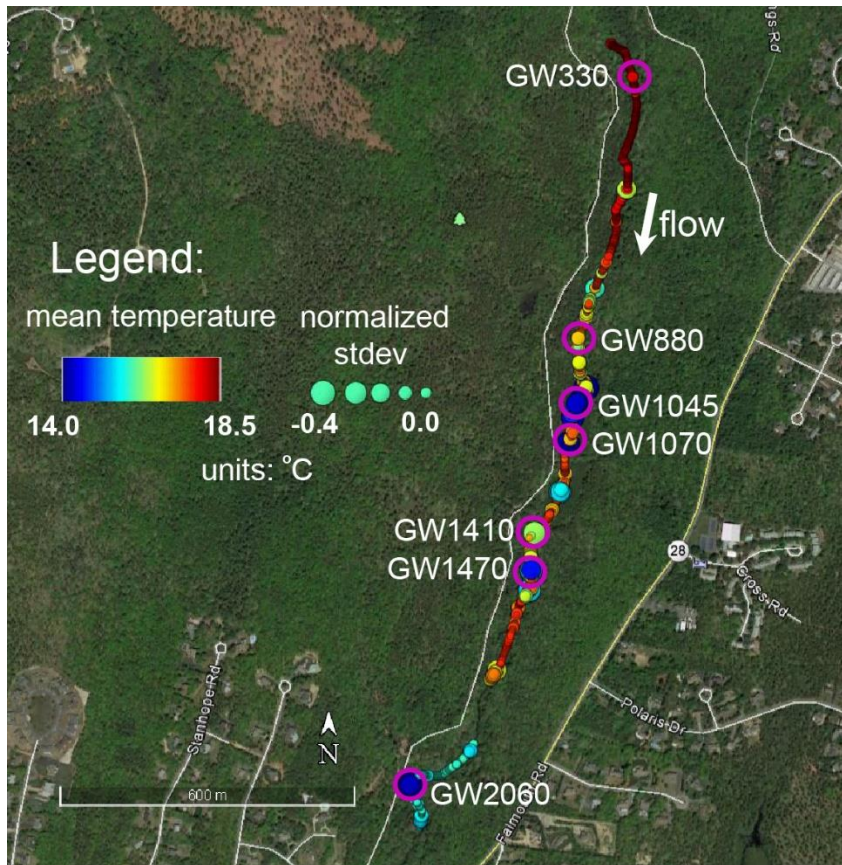


Figure 1. Streambed interface temperature data were collected over time to indicate preferential groundwater discharge zones using reduced thermal variance and relatively cold mean temperature metrics. Apparent streambed discharge zones with a range of temperature characteristics were directly sampled for dissolved oxygen, specific conductivity, and stable water isotopes, and labeled as downstream distance from a common upstream point (e.g. GWxxxx from the fish ladder). This Figure is modified from Rosenberry et al. (2016).

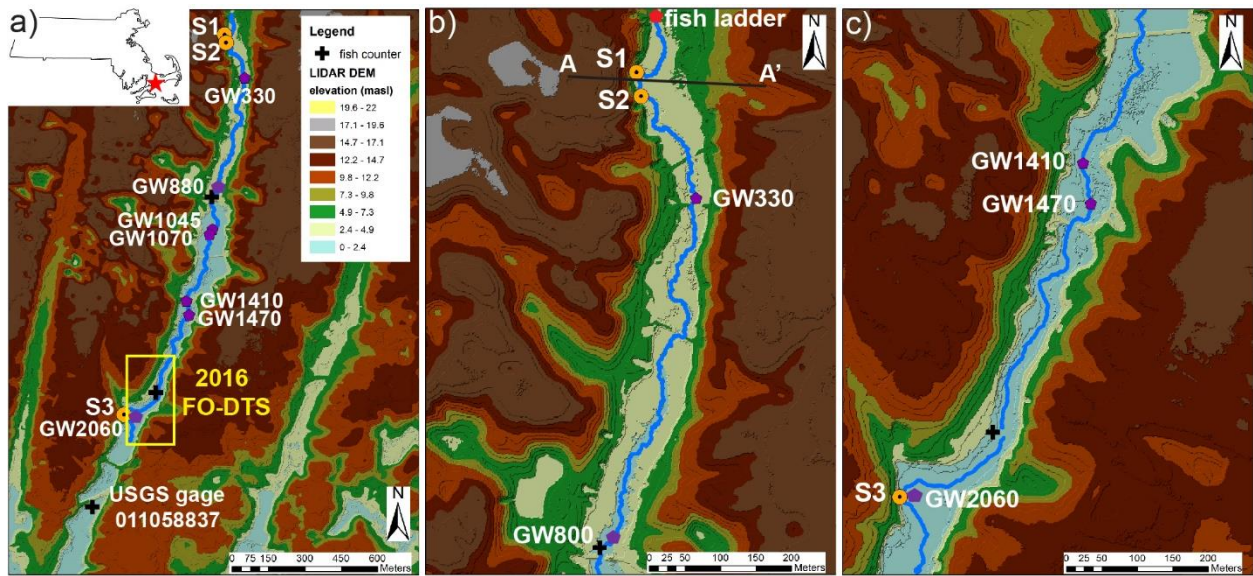


Figure 2. Lidar elevation data show the linear valley terrain of: a) The lower Quashnet River reach with Spawn (S1, S2, S3) locations and major open valley seepage zones identified. All seepage zones are labeled as downstream distance from the stream crossing/fish ladder located at the upper extent of this image. Panel b) shows the tighter upper valley zone where Spawn 1 and 2 are located at the base of a steep cut bank and the topographic transect of Figure 1 is noted. Panel c) displays the lower open valley reach where Spawn 3 is located along a cut bank.





Figure 3. Images collected in February 2016 a) the cut bank alcove at Spawn 1, b) open valley seepage GW1045, and c) fresh cut bank slumping and visible seepage Spawn 3. Panel d) is an image from the underwater video collected in fall 2015 of spawning trout in the Spawn 1 alcove pictured in panel a), showing several fish clustered around the sandy zone directly at the base of the cut bank.



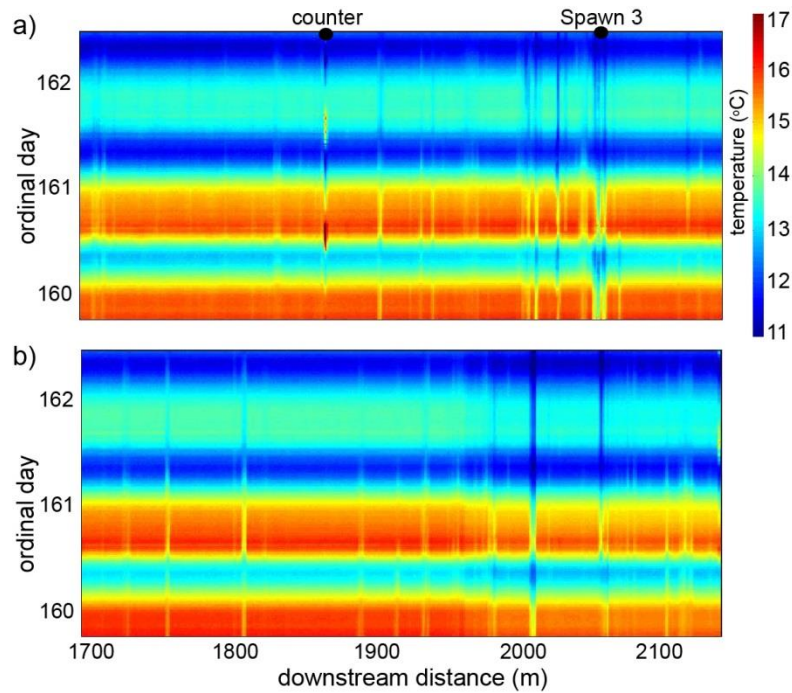


Figure 4. Fiber-optic-distributed temperature data collected from approximate channel distance 1700 to 2160 m along a) the downstream right bank through the Spawn 3 meander bend area (see Figure 2c for location), and b) the downstream left bank. The persistent vertical bands of relatively cool temperatures indicate discrete groundwater discharge. Some larger zones display a thermal signature on both bank cables, while smaller discharges may be bank-specific.

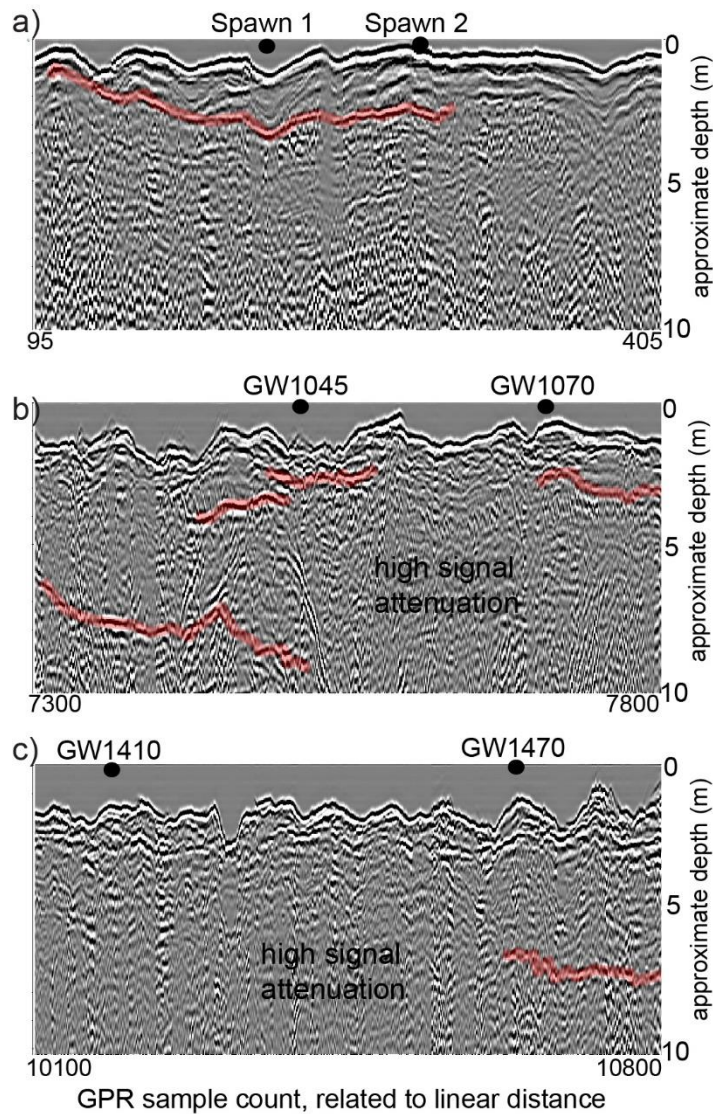


Figure 5. Quashnet River thalweg ground penetrating radar profiles were collected in the vicinity of: a) Spawn 1 and 2; b) open valley seepage GW1045 and GW1070; and c) open valley seepage GW1410 and GW1470. Stronger apparent reflectors are highlighted in red, and likely indicate sediment layer boundaries (e.g. sand/gravel and peat).

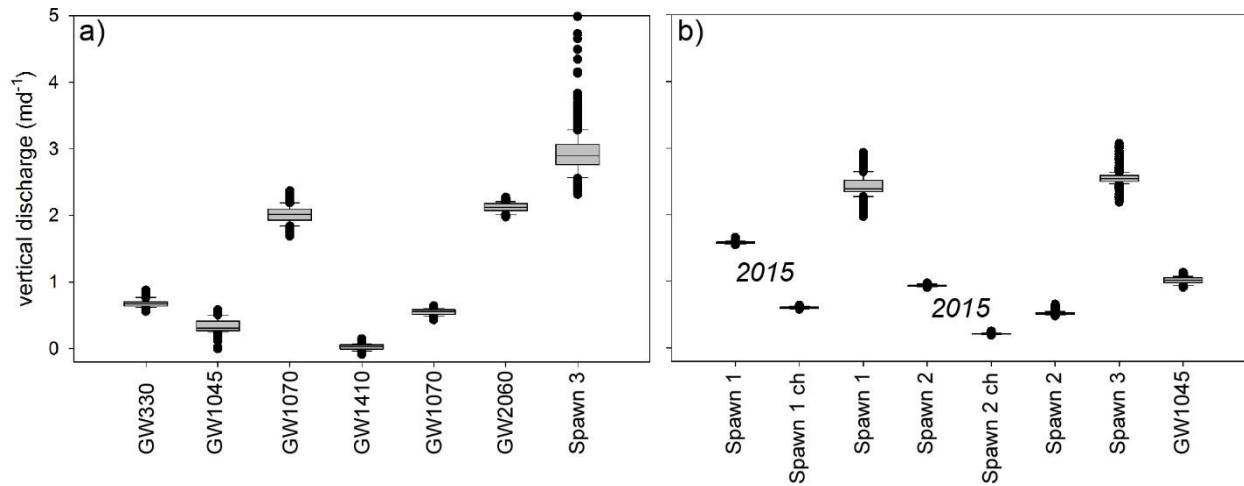


Figure 6. Panel a) displays summary box plots of sub-daily (June 11 to July 13, 2014) vertical groundwater discharge rate estimates for the open valley discharge and Spawn 3 bank locations. Panel b) shows vertical discharge rates collected against the banks and toward the channel at Spawn zones 1 and 2 (August 21 to September 13, 2015); and from locations against the bank in all three Spawn locations and GW1045 (June 5 to July 9, 2016).

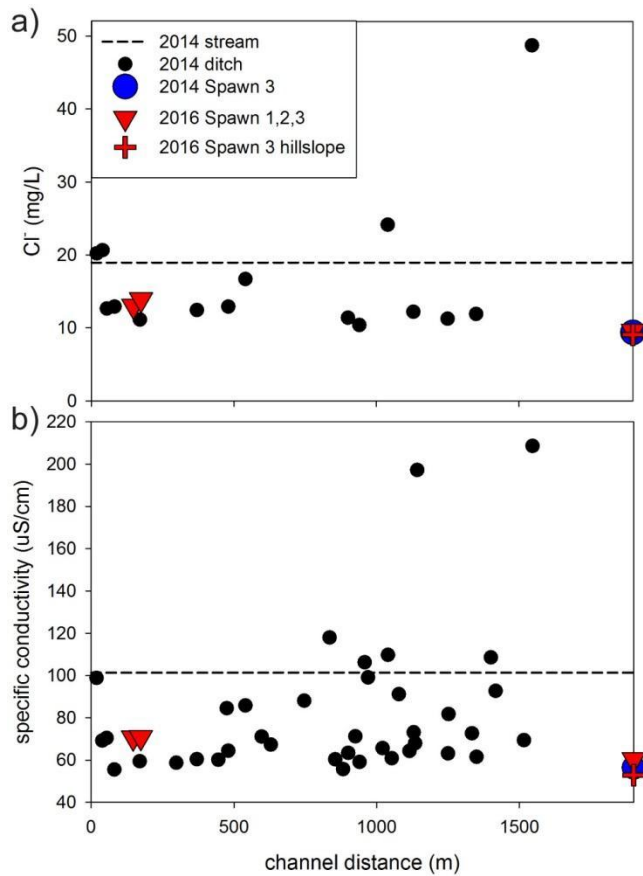


Figure 7. Drainage ditch chemistry throughout the lower Quashnet showing a)  $\text{Cl}^-$ , and b) specific conductance, collected in June 2014 just above the confluence with the main channel. Data are plotted as distance from the upper flood control structure in the narrow valley reach and compared to groundwater seepage data collected in preferential spawning locations and a hillslope piezometer.

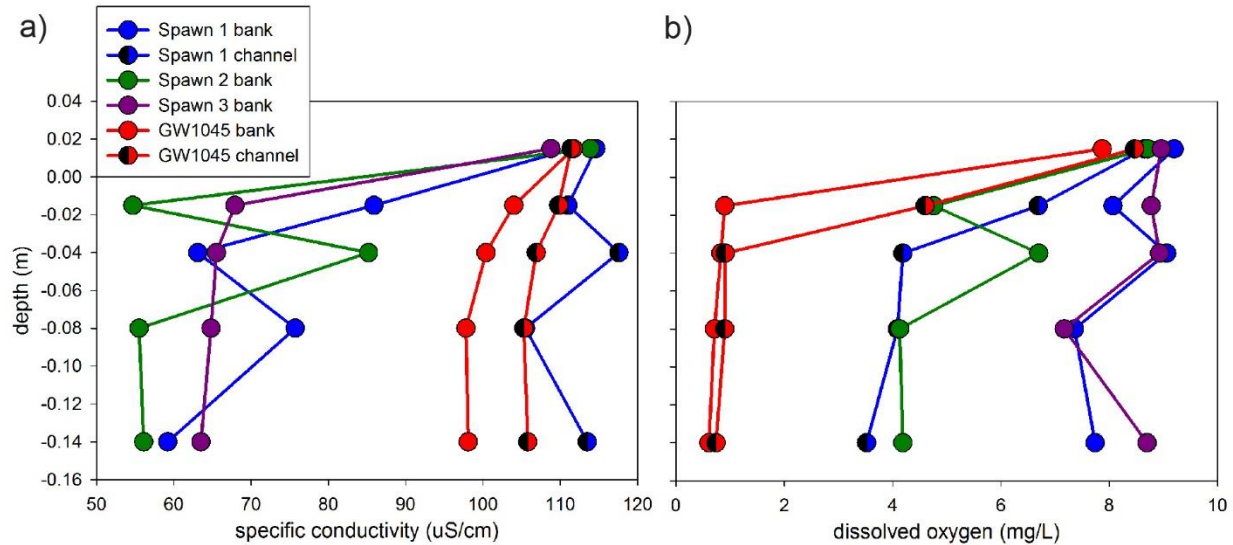


Figure 8. Minipoint pore-water chemistry data showing high spatial resolution profiles of a) specific conductance, and b) dissolved oxygen, collected in June 2016 at the major seepage alcoves. Triangle symbols indicate data collected farther toward the thalweg from the respective alcove bank, and all profiles include a local stream water sample taken just above the streambed interface.

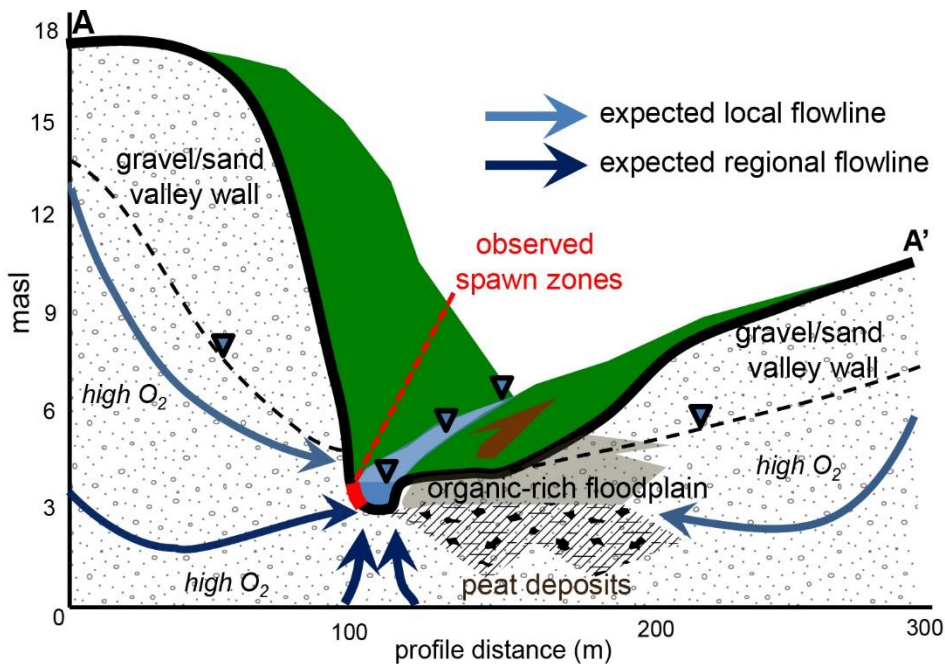


Figure 9. Based on previously published USGS work (e.g. Modica, 1999; Winter et al., 1998), the conceptual model in panel a) displays how groundwater discharge to lowland streams is expected to include locally sourced lateral groundwater discharge through valley wall features and more regionally sourced groundwater discharge vertically through the streambed. The topographic profile shown here (A-A') is derived directly from lidar data in the vicinity of observed preferential brook trout spawning habitat shown in Figure 2. In contrast to the sand and gravel valley walls, multiple methodologies used for this study indicate wider valley zone sediments to be rich in organic material, including buried peat deposits, consistent with known

944 regional geology.

945

946 **Supplemental**

947

948 Supplemental Video S1. Underwater video of brook trout spawning in the fall of 2015 (still

949 image Figure 3d).